Energy Equipment and Systems

Simulation of fouling effects on a two-stage axial turbine performance

Authors

Hadi karrabi[a]
Ali Samaeenia[b]
Abolhassan Asgarshamsi[c]
Mostafa Baghani[d]*

[a] MAPNA Turbine Engineering and Manufacturing Company (TUGA)

[b] School of Mechanical Engineering, Hakim Sabzevari University, Sabzevar, Iran

[c] Department of Mechanical Engineering, Golpayegan College of Engineering, Isfahan University of Technology, Golpayegan 87717-67498, Iran

[d] School of Mechanical Engineering, College of Engineering, University of Tehran, Tehran, Iran

ABSTRACT

The axial turbine is one of the most important components of gas turbines in industrial and aerospace applications. As time passing the increasing of the roughness of the axial turbine blades is unavoidable. The aim of this paper is numerical investigation of the blades roughness effects on the flow field and performance of a two-stage axial gas turbine. In this research, the axial turbine is simulated three-dimensionally and the results are validated with experimental data. Then, the effects of blade roughness on flow field and performance of the turbine are investigated in five different pressure ratios. Also, in order to determine the role of stators and rotors roughness in decreasing the turbine efficiency, in a specific roughness, the first and second stators and then the corresponding rotors have been simulated separately. Numerical results show that the efficiency drop in the turbine stage is approximately equal to summation of efficiency drops when the roughness effect on the stator and rotor blades is applied, separately.

1. Introduction

Gas turbine blades due to use in specific conditions are damaged by various factors such as hot corrosion, oxidation, external particle collisions, sediments of impurities and sticking of dust. The surface roughness of the blades increases because of these factors. In recent years, use of computational fluid dynamics in simulation of turbo-machinery has grown significantly. Numerical analysis tools in analyzing turbomachinery flows have been employed widely in several researches like Thakker [1], Hudson [2], Aghaei et al [3, 4].

An investigation on the effect of roughness on boundary layer of turbulent flow and its possible impact on the transient flow was conducted by Fiala et al [5]. Strip et al [6] studied the effect of surface roughness on the secondary flow. In their study, eight types of blades with different roughness and a smooth surface as a reference were investigated.

The effect of different roughness on the efficiency and work coefficient of a turbine using CFX task flow software were explored by Young Seok Kang et al [7] where the results

---
* Corresponding author: Mostafa Baghani
School of Mechanical Engineering, College of Engineering, University of Tehran, Tehran, Iran
E-mail address: baghani@ut.ac.ir

were compared with those of experimental data. The computed results showed that the pressure ratio and efficiency has been reduced by the roughness of the blades. The total loss of efficiency because of the rough rotor and rough stator was approximately equivalent to the loss of efficiency due to the total stage roughness. They concluded that the effect of surface roughness on the secondary flow near the side walls was considerable.

Frank Hummel et al [8] investigated the effect of roughness on the blade aerodynamics. In this study, four different roughness values were applied on the blades for Reynolds numbers between 600,000 and 1,200,000. The obtained results revealed that in higher Reynolds numbers, the pressure loss increases with increasing friction. Also the maximum total pressure loss is generated at the highest Reynolds number and its value is 40 percent higher than the smooth blade. Comparison of the obtained results with similar studies, were shown good agreements

The sources of losses in turbine blades are as follows: profile loss (due to figure of blade, boundary layer and skin friction), rotor blade tip clearance loss (the flow leakages from the pressure side to suction side of the rotor blade) and loss of the secondary flows in wall boundary layers.

In Previous studies, the research that includes experimental or numerical analysis on the effects of roughness or even sediment and corrosion, either separately or simultaneously on all stages of a multistage turbine, the current turbine and also the turbine with cooling has not been done.

In this study, the turbine geometry and its boundary conditions are modelled and then validation is done. Then the turbine performance is analyzed in various and actual roughness conditions.

Nomenclature

E	Energy
H	Actual power of the turbine
P	Static average pressure
∇P	Pressure variation
T	Temperature
t	time
u	Linear velocity of blade

U	Velocity
C_0	Absolute fluid velocity
C_P	Specific heat capacity at constant pressure
u_i	Velocity components
η	Efficiency
W_1	Relative velocity of the fluid at stator outlet
w_c	Mass flow rate of cooling fluid
ρ_c	Density of cooling fluid
ρg	Body force of gravity
Δh_a	Isentropic enthalpy variations
$\dot{m}_{inlet}$	Inlet mass flow rate
$\dot{m}_{outlet}$	Outlet mass flow rate
$P_{0,inlet}$	Inlet total pressure
$P_{0,outlet}$	Outlet total pressure
P_{0rel}	Relative total pressure
H_{R1}	Actual power of the first stage of the turbine
H_{R2}	Actual power of the second stage of the turbine
n	Number of mesh elements
$K^+{}_{eq}$	Roughness Reynolds number
h_{inlet}	Inlet enthalpy
h_j	Enthalpy tensor
h_c	Coolant enthalpy
P_{01}	Stagnation pressure at stator inlet
$P_{t,c}$	Total pressure of cooling fluid
P_{ti}	Total pressure at turbine inlet
P_{to}	Total pressure at turbine outlet
T_0	Total temperature
$T_{t,inlet}$	Inlet total temperature
T_{so}	Static temperature at turbine outlet
$\Delta h_{a,c}$	Coolant Isentropic enthalpy variation
η_{exp}	Experimental efficiency
η_{CFD}	Numerical efficiency
η_{TH}	Thermodynamic efficiency
μ	Molecular viscosity of the fluid
m^0	The turbine mass flow rate
$\dot{m}_c$	Mass Flow rate of cooling fluid
ν	Kinematic viscosity
Y_S	Stator loss coefficient
Y_R	Rotor loss coefficient
T_{0i}	Inlet total temperature
T_{0o}	Outlet total temperature
$T_{t,41}$	Outlet total temperature of first rotor
Y^+	Non-dimensional wall distance
N	Turbine rotational speed
U_τ	Friction velocity
K_{eq}	Sand-grain roughness

2. Governing equations

I order to analyze the characteristics of all streams, mass and momentum conservation equations have been solved. For compressible flows or flows involving heat transfer, energy conservation equation is also solved. When the flow is turbulent, turbulence modelling equations should be used. The purpose of modelling turbulent flows is determination of Reynolds stress, turbulent mass flux or turbulent heat flux using relation between the values of mentioned quantities to the gradient of the mean flow quantities.

In this study, shear stress transport (SST) model is used for turbulence modelling. This model has high performance to observe near-wall and secondary flows. Calculated results of this model are shown significant progress in the field of flow separation. The high performances of this model have been shown in significant numbers of studies [7, 9].The SST model is suggested to simulate the boundary layer with high accuracy [10].

2.1. Continuity equation

Continuity Equation or conservation of mass is written as follow:

$$\frac{\partial \bar{\rho}}{\partial t} + \frac{\partial}{\partial x_i}\left(\overline{\rho u_i}\right) + \frac{\partial}{\partial x_i}\left(\overline{\rho' u_i'}\right) = 0 \qquad (1)$$

In this Equation, ρ is fluid density and u_i is velocity component.

2.2. Momentum equation

Momentum Equation in general form is as follow:

$$\rho \frac{D\bar{V}}{Dt} + \rho \frac{\partial}{\partial x_j}\left(\overline{\rho u_i' u_j'}\right) = \rho g - \nabla \bar{P} + \mu \nabla^2 \bar{V} \qquad (2)$$

In Eq.(2), $\bar{P}$ is average static pressure and ρg is body force of gravity that its value is negligible in this research.

2.3. Energy equation

Energy Equation can be stated as follow:

$$\rho C_p \frac{D\bar{T}}{Dt} = -\frac{\partial}{\partial x_i}\left(-k\frac{\partial \bar{T}}{\partial x_i} + \rho C_p \overline{u_i' T'}\right) +$$
$$\frac{\mu}{2}\left(\frac{\partial \overline{u_i}}{\partial x_j} + \frac{\partial u_i'}{\partial x_j} + \frac{\partial \overline{u_j}}{\partial x_i} + \frac{\partial u_j'}{\partial x_i}\right)^2 \qquad (3)$$

The $\rho C_p \overline{u_i' T'}$ term is the correlation between velocity and temperature fluctuations and represents the transition of enthalpy in the x_i direction. These equations are so-called RANS[1] equations.

3. Used Parameters

Parameters that are used to compare the performance of normal and defective turbines are:

1. Thermodynamic efficiency or ratio of total efficiency to total isentropic efficiency that considering the complete cooling of blades by the cooling holes is defined in Eq.(4). In this equation, H is actual power of the turbine and is obtained from the Eq.(5) [7]:

$$\eta_{TH} = \frac{H}{w_{41}\Delta h_a + \sum w_c \Delta h_{a,c}} \qquad (4)$$

$$H = \underbrace{\dot{m}_{inlet} h_{inlet} + \dot{m}_c h_c - \dot{m}_{outlet} h_{outlet}}_{H_{R1}}$$
$$+ \underbrace{\dot{m}_{inlet} h_{inlet} + \dot{m}_c h_c - \dot{m}_{outlet} h_{outlet}}_{H_{R2}} \qquad (5)$$

The denominator of Equation (4) is the ideal power in the isentropic condition and the w_{41} term is the inlet mass flow of first rotor, w_c is the related mass flow of cooling fluid, Δh_a and $\Delta h_{a,c}$ are the difference in actual enthalpy of the working fluid and cooling flow, respectively.

2. Loss coefficients due to the stator and rotor losses are calculated from Eqs.6 and 7.

$$Y_S = \frac{P_{01} - P_{02}}{P_{01} - P_2} \qquad (6)$$

$$Y_R = \frac{P_{02,rel} - P_{03,rel}}{P_{03,rel} - P_3} \qquad (7)$$

That P_{01} and P_{02} are inlet and outlet total pressure to stator or rotor, respectively and P_2 is outlet static pressure. Also $P_{02,rel}$ and $P_{03,rel}$ are relative pressure of the inlet and outlet of the rotor respectively and P_3 is rotor outlet pressure.

3. The drops in total pressure and total temperature at the turbine stage are:

---

1. Reynolds Averaged Navier-Stokes

$$Pd = \frac{P_{0i} - P_{0o}}{P_{0i}} \qquad (8)$$

$$Td = \frac{T_{0o} - T_{0i}}{T_{0i}} \qquad (9)$$

That in Eqs. (8, 9), P_{0i} and P_{0o} are inlet and outlet total pressure respectively also T_{0i} and T_{0o} are inlet and outlet total temperature of turbine, Pd is the total pressure drop and Td is total temperature drop.

4. Numerical Simulation

To investigate, a two-stage axial turbine, the E^3 turbine, is considered. This turbine is manufactured by General Electric Company and is used in the aerospace Industry. The purpose of GE was technological development in order to improve the efficiency of propulsion systems for commercial subsonic aircraft that was

performed in January 1978. Turbine laboratory equipment includes a full-scale two-stage high pressure axial turbine with complete cooling. Equipment is predicted for measuring fluxes, temperatures, shaft speed, torque and outflow angle. The general specifications of the turbine stage are given in Table 1.

The process of three-dimensional simulation, include three basic steps: geometry generation, mesh generation and fluid analysis.

4.1. Axial turbine geometry

In Fig. 1, a two-dimensional schematic of the turbine geometry is shown. Also the three-dimensional view of the studied turbine is displayed in Fig. 2. Using the coordinates of the points which is completely considered at NASA report, the geometry of the blades are shaped in Blade Generation software.

Table 1. Specifications of the E^3 turbine [11]

| Specification	Quantity
Inlet total pressure to outlet static pressure	5.55
Rotor design point speed	8283 rpm
Number of first stator blade row	46
Number of second stator blade row	48
Number of first rotor blade row	76
Number of second rotor blade row	70
First rotor blade tip clearance	0.0427 cm
Second rotor blade tip clearance	0.04188 cm
Inlet total temperature	709.44 K
Inlet total pressure	344.7 kPa
Outlet static pressure	62.108 kPa
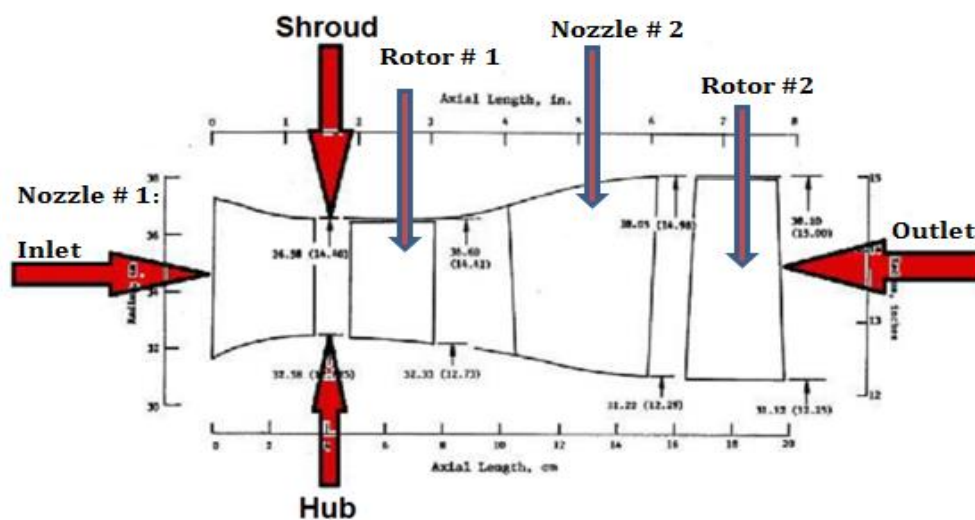
Fig. 1. Schematic of the studied turbine.

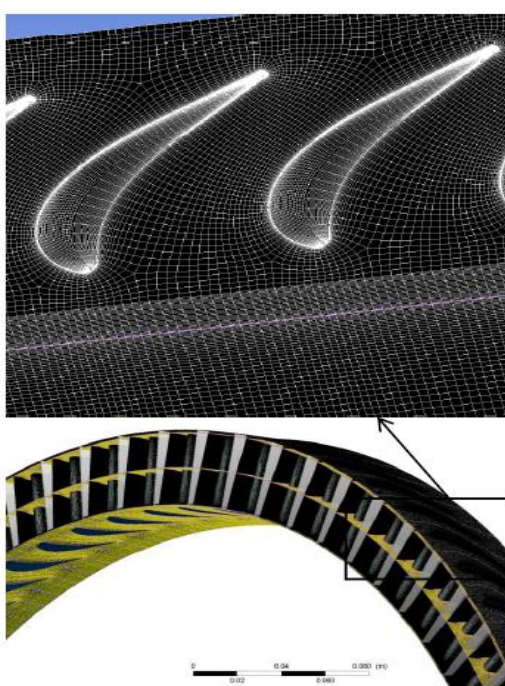**Fig. 2.** Three-dimensional geometry of the E3 turbine.

Fig. 3. Elements of the blades with concentration on boundary layer.

4.2. Grid generation

One of the most important steps of three-dimensional analysis is mesh generation. The elements are appropriate that have been small enough in places with intense gradients. Therefore the mesh size selection required a balance between accuracy and computational time. This step is almost a process based on trial-and-error method. In Fig.3 the elements of first rotor blades are shown. The small elements around the edges of the blade are perfectly specified.

4.3. Grid independency

Using small mesh elements, errors of numerical methods are reduced and the computational time is greatly increased. In order to obtain independent results from the grid size and achieve high accuracy, several mesh sizes are used to calculate the efficiency and pressure ratio [8-9, 12]. As shown in Fig. 4 and 5, from specific number of elements, efficiency and pressure ratio are not changed significantly. The number of final elements is more than 1900000.

Details of number of elements that is used in the analysis of rotors and stators and actual y^+ in boundary layer of second rotor blades are given in Table 2.
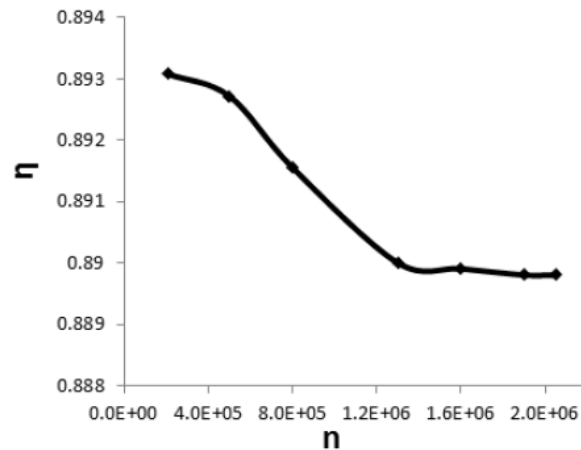
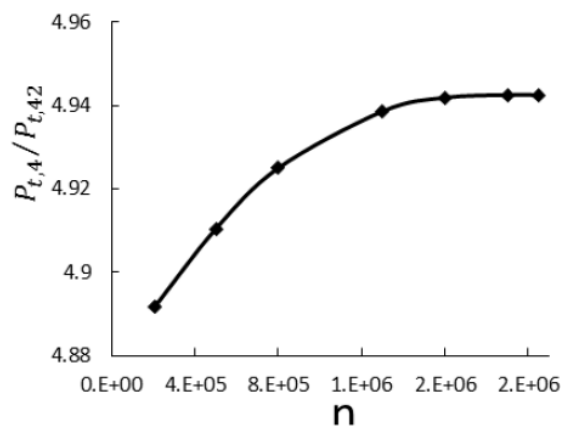**Fig. 4.** Grid independendency analysis based on the turbine efficiency.

Fig. 5. Grid independendency analysis based on the turbine pressure ratio

Table 2. Elements number of turbine blades and actual y^+ in boundary layer of second rotor blades

Actual y^+	Number of rotors elements	Number of stators elements	Total number of elements
99.566	117814	87278	205092
66.6517	295034	205024	500058
66.6517	441549	358634	800183
20.1955	692386	608292	1300678
20.8187	912581	683738	1596319
20.1955	985403	922653	1908056
18.9619	1051039	998872	2049911

Table 2 Elements number of turbine blades and actual y^+ in boundary layer of second rotor blades

The boundary conditions of all simulation; are included [9]:

1. At inlet of the nozzle, total pressure boundary condition is used. Flow direction at the entrance is assumed perpendicular to the inlet surface (with no pre-whirl). The average total temperature and turbulence intensity as input parameters have been applied.
2. The average static pressure at the outlet of second rotor is used as an output boundary condition.
3. The adiabatic boundary condition for all stationary and rotating walls and no-slip condition for velocity on the surface are assumed.
4. The interface boundary condition between

the rotor and the nozzle of first and second stage is defined as mixing plane.

5. Because the turbine has axial symmetry, the periodic boundary condition for the rotor and nozzle are used. This means by using periodic boundary condition only one rotor and nozzle blade are simulated.

The use of periodic boundary conditions and other boundary conditions are shown in Fig. 6. Also the implementation of cooling holes is visible.

Figure 6 View of three-dimensional blade to blade with cooling holes and imposed boundary conditions.

The film cooling is applied with the air as an ideal gas. The holes are circular with different areas [12]. In Tables 3 and 4, the flow rates and temperatures of the cooling fluid and entrance fluid to turbine are presented. Due to the entrance of hot gas that its high temperature is one of the destructive factors and consequently caused roughness in the blades, the maximum number of holes are allocated in the first stator specially in the leading and trailing edges which are needed more cooling. In Table 3, the turbine inlet flow rate of combustion products and also rate of cooling air in holes of stators and rotors, with different pressure ratios are given for healthy turbine. Inlet temperature of working fluid and cooling air can also be seen in Table 4.
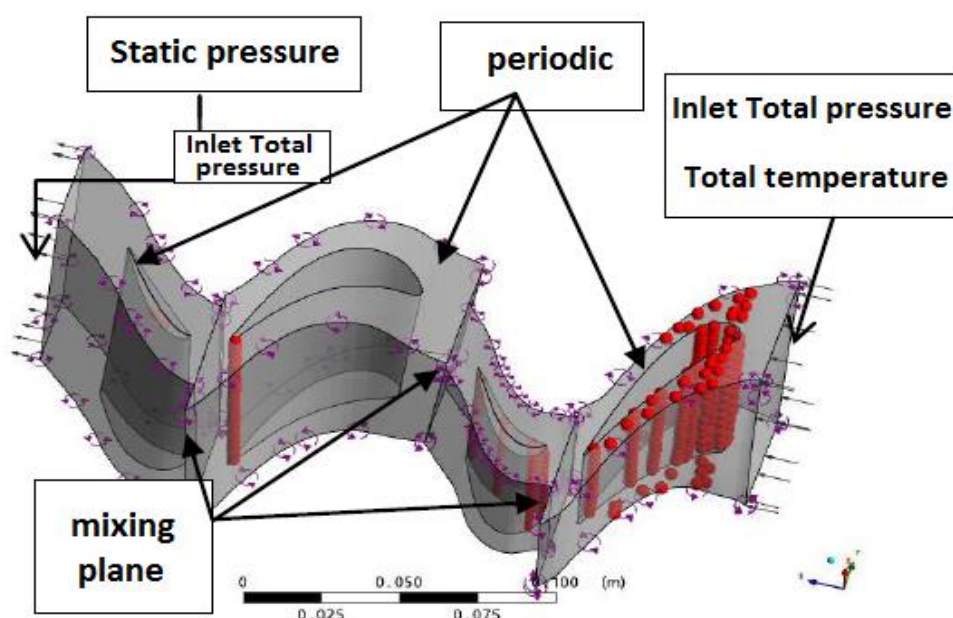

Fig. 6. View of three-dimensional blade to blade with cooling holes and imposed boundary conditions.

Table 3. Mass flow rates at turbine inlet and cooling holes in design point (kg/s)

Holes of the rotors	Holes of the second stator	Holes of the first stator	Turbine inlet	Pressure ratio
0.4129	0.8579	1.8185	14.8376	8
0.3654	0.7365	1.5798	12.9646	7
0.2817	0.5875	1.2738	20.2318	5.5
0.1919	0.40255	0.8736	7.0187	4
0.1086	0.2285	0.4828	4.5715	2.5

Table 4. Fluids temperature at turbine inlet and cooling holes (K)

Holes of the rotors	Holes of the second stator	Holes of the first stator	Turbine inlet
300	344	352	709.444

In actual operating conditions, the boundary conditions of 1 and 2 changed to stagnation temperature 709 K. As well as five different inlet total pressures and atmospheric static average pressure at outlet are changed.

Working fluid is combustion products and the flow is assumed steady, compressible and subsonic. The combination of combustion products is used instead of ideal air that its combination is given in right hand side of Equation 10. On this basis, methane has reacted with 191 percent of extra air [12].

$$CH_4 + 5.82(3.76N_2 + O_2) \rightarrow$$
$$CO_2 + 2H_2O + 21.92N_2 + 3.82\, O_2 \quad (10)$$
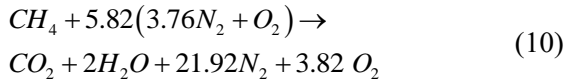
5. Validation of Numerical Results

For validation, obtained curves from laboratory measurements have been studied for velocity ratio $\frac{U}{C_0}$, turbine efficiency and ratio of inlet to outlet total pressure (Fig. 7 and 8). In the design point, the ratio of corrected velocity is $\frac{N}{\sqrt{T_{inlet}}} = 236.2 \quad rpm/\sqrt{K}$ and velocity ratio is $\frac{U}{C_0} = 0.575$.

The percentage of efficiency error is an appropriate certificate to validate the computational results.

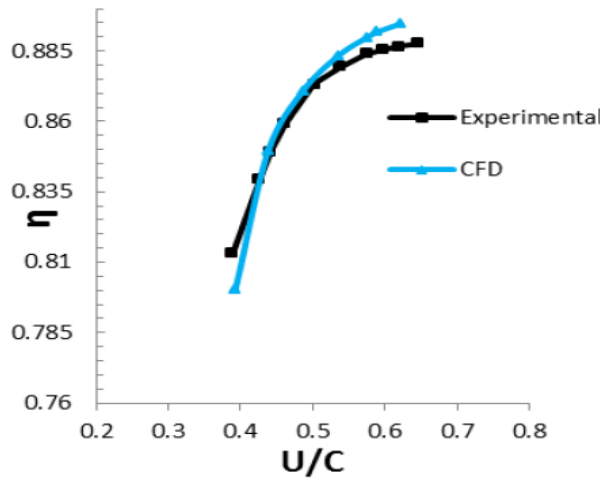$$\begin{cases} \eta_{exp} = 88.4\% \\ \eta_{CFD} = 88.98\% \end{cases} \rightarrow Relative\ Rror = 0.65\%$$

Fig. 7. Experimental and numerical turbine efficiency versus velocity ratio $\frac{U}{C_0}$.
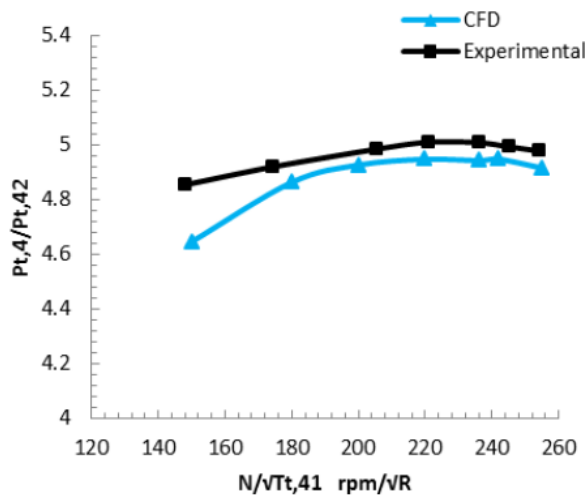

Fig. 8. Experimental and numerical total pressure ratio versus corrected velocity.

Generally appropriate adaptations are observed between experimental data [12] and numerical solutions.

6. Defective Turbine modelling

In this section, defective turbine will be discussed.

6.1. Roughness

Roughness values are used in the previous numerical analysis [7, 13], 100 μm, 300 μm and 500 μm are, in the region of transition roughness, shortly after the transition (at beginning of completely rough zone) and fully rough, respectively. Also usual roughness provides a better comparison of the results. To obtain the effect of rotor and stator roughness on turbine performance and for the case of 300μm, once only the first and second stators, then their corresponding rotors and finally, all the blades were roughened 300μm. The height of the first elements adjacent to wall are considered equal to roughness height. Turbulence intensity at inlet defined 5% and SST turbulence model is used [12]. In CFX software to define the roughness value there is an item as equivalent height of sand grain [14].

6.2. Roughness regimes

Three types of flow regime for turbulent flow near the wall are expressed as follows [15]:

Smooth region: In this case, there is not any effect of roughness on the flow. In other words, the pipe friction coefficient is a function of average Reynolds number of flow. Based on hydrodynamic and aerodynamic, this regime is called smooth.

$$K_{eq}^{+} = U_{\tau} \frac{K_{eq}}{\nu} \leq 5 \qquad (11\text{-}a)$$

Transition region: an increase in flow resistance is observed. This condition is related to the prominence of roughness elements when covered viscose sublayer.

$$5 \leq K_{eq}^{+} = U_{\tau} \frac{K_{eq}}{\nu} \leq 70 \qquad (11\text{-}b)$$

Rough region: a greater increase in flow resistance is observed. This regime is called, fully rough regime and specially is created when the prominence size of the roughness is much larger than viscous sublayer and transition zone.

$$K_{eq}^{+} = U_{\tau} \frac{K_{eq}}{\nu} \geq 70 \qquad (11\text{-}c)$$

7. The Numerical results

In this section, roughness effects on flow field and turbine performance are investigated numerically.

By increasing roughness, friction and thickness of boundary layer are increased. Both of these factors increase profile loss. In addition to increase the profile loss, thicker boundary layer on the blades and the side walls, reduce flow capacity especially near the choking condition. The effect of the boundary layer can be seen in Fig. 9 and 10.

Applied roughness of turbine covered blade surfaces, shroud, hub, and casing of turbine. Boundary layer especially on the suction side of the rough blade is thicker than smooth blade and roughness causes irregular flow lines around the blade and as shown in Fig. 9, irregular flow especially in the stator blades is expanded. Consequences of this case are lack of complete energy transfer of flow to rotor blades and undesirable recovery of flow velocity in the stator and so, reduce the efficiency of the turbine. Surrounding the stator blades, irregular distribution of flow is more than rotor blades because of rotor blades are being rotated and flow friction is reduced with blade surface.

The boundary layer is affected extremely that this condition is clearly detectable by observation in Fig. 10 and comparison with Fig. 9. Flow at the trailing edge of the blade is also strongly influenced by the roughness.

This region is responsible for flow transfer from blade to blade .If the flow is not passed from its ideal path, at the entrance to the other blade, the stagnation point at the leading edge, and then desired direction of flow are impressed and changed. This phenomenon is the reason of increasing influence of roughness on the second stage of blades in comparison with the first stage (Fig.11).

In Fig.12, changes in flow behavior due to roughness on trailing edge of second stator blade is clearly visible.

Based on above discussion, the entropy distribution is increased by increasing roughness. In Fig.13, the effect of roughness on the total entropy distribution of turbine is shown in side view.
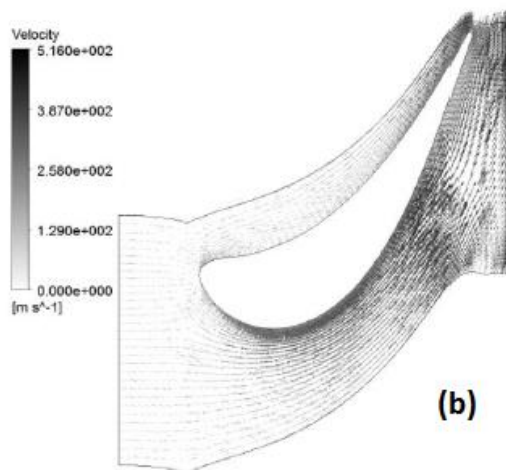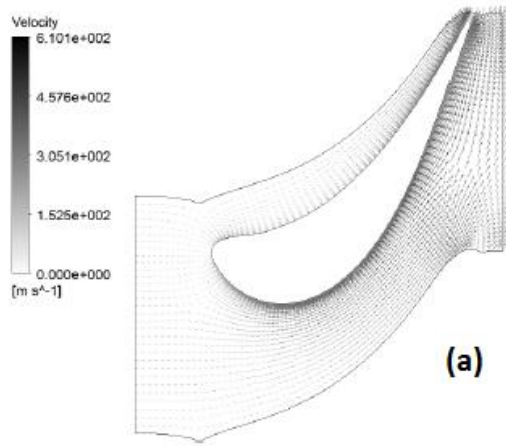

(a)

(b)

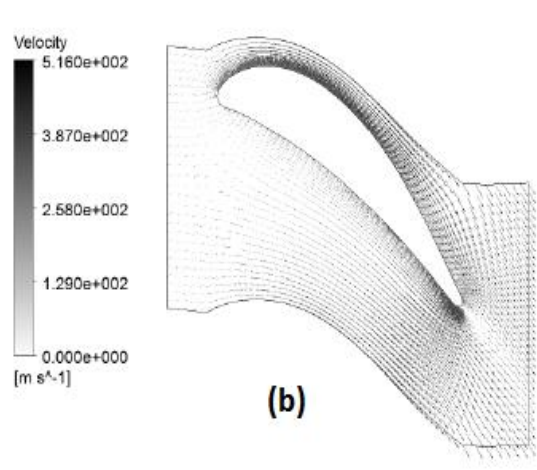**Fig. 9.** Velocity vectors of second stator blades: for smooth (a) and rough surface (b) at mid-span of the blade.

(a)

(b)
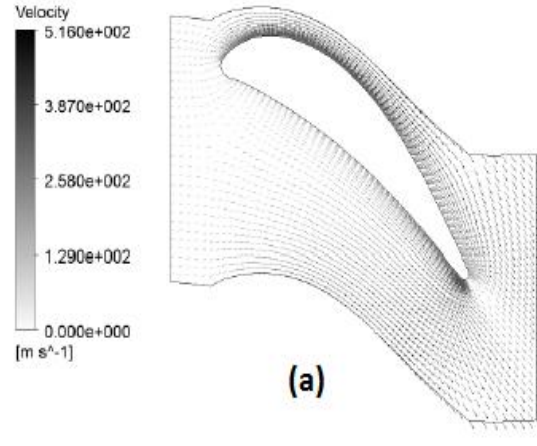
Fig. 10. Velocity vectors of second rotor blades: for smooth (a) and rough surface (b) at mid-span of the blade.
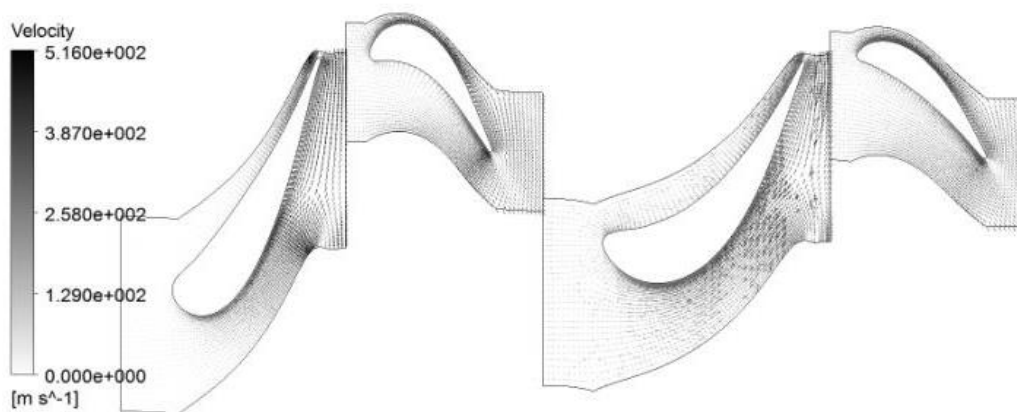

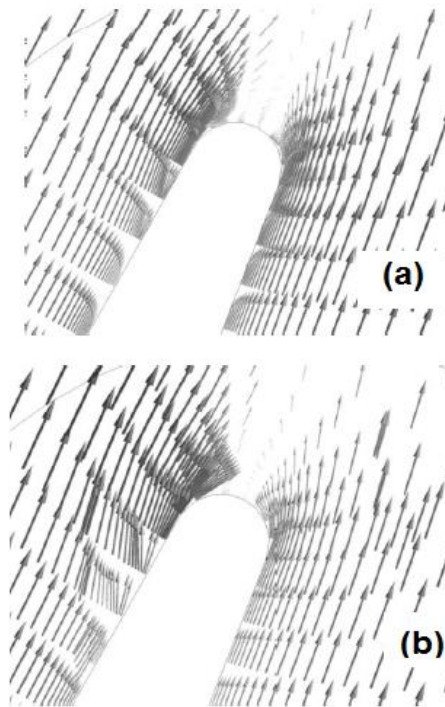**Fig. 11.** Blade to blade view of the turbine for the rough mode.

Fig. 12. The velocity vectors on trailing edge of second stator blade: for smooth (a) and rough surface (b) at mid-span of the blade.
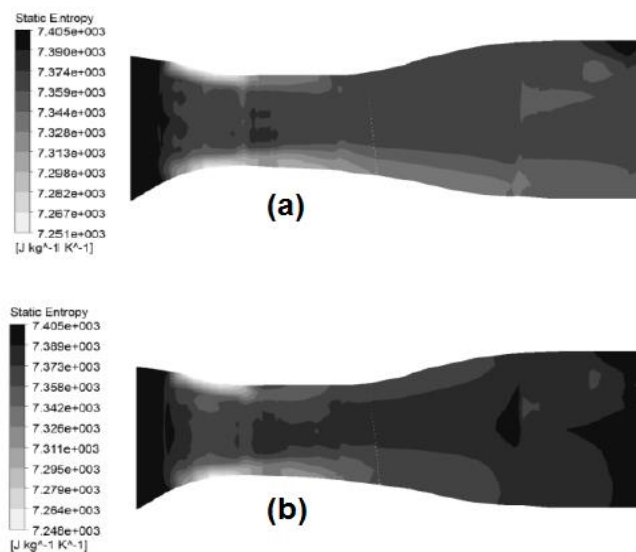

Fig. 13. Entropy distribution in entire turbine for smooth (a) and rough surfaces of both stages (b).

Increasing in entropy and moving away from the desired flow in comparison with normal condition, is appeared clearly, especially in the boundary layer at the suction side of rough blade and at the outlet and inlet of second rotor (outlet region of defective turbine). Increase in heat transfer due to increase molecular interactions at the end of defective turbine in comparison with normal turbine, is one of the influential factors of increasing entropy.

In Fig. 14 variations of inlet mass flow with different achievable pressure ratios, for smooth turbine and rough turbine with 100, 300 and 500 microns roughness, are shown [12].
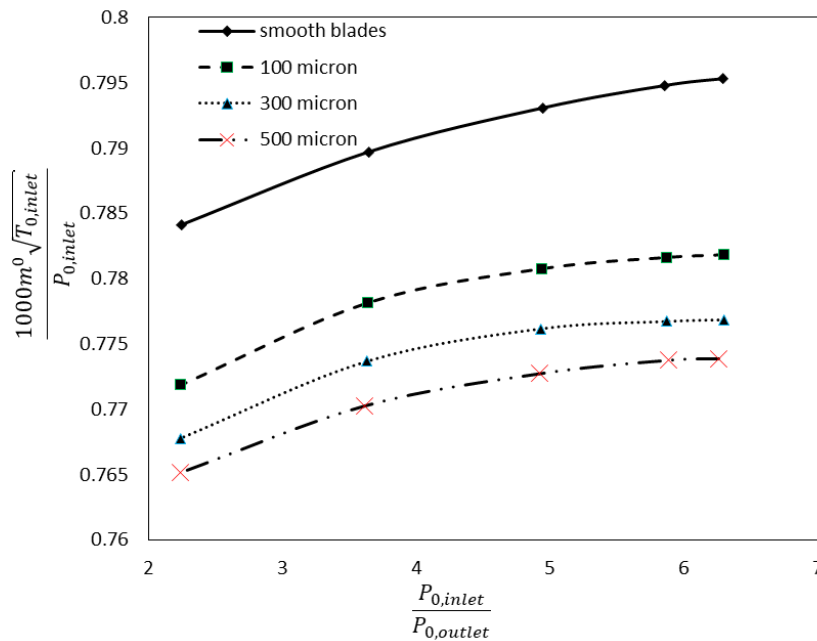
Fig. 14. Curves of reduced mass flow rate versus total to total pressure ratio, for different roughness values.

According to the above curve, by increasing pressure ratio, the flow rate will be increased as expected, whatever pressure ratio increases, the amount of increased flow is reduced until due to the choking phenomenon will be constant. The notable issue is access this condition more quickly by increasing roughness because according to Fig.14, the slope of curve decreases by increasing roughness.

Also by increasing roughness, the inlet mass flow will be reduced, because by increasing irregularity of flow and disturbances caused by the roughness; flow velocity through the turbine especially at the inlet of first stator is decreased slightly and will be caused increasing in local pressure so the difference between local pressure and inlet pressure is reduced and the flow rate is also reduced. This trend will be continued by increasing roughness, but it was observed that this reduction in mas flow rate will not be with constant ratio.

Roughness and defect of turbine will affect the inlet flow rate to the cooling holes. It will be cleared by comparing Tables 4 and 5 when the pressure ratio is 5.55.

In Fig. 15 and Table 6, the efficiency for five different actual pressure ratios and for different roughness, have been compared. Since in a rough mode, roughness elements are outside of the viscose sub-layer and create drag and additional resistance, the friction increased greatly. Also the thickness of the boundary layer is increased and causes increase in profile loss. The efficiency is reduced by both of these phenomena, but reduction of efficiency such as reduction of inlet mass flow, cannot be in constant trend with increasing roughness because by creation of required roughness to reach turbulence of boundary layer to transition condition, significant decrease in the efficiency and flow rate will be created. By reaching the fully rough region, the thickness of the boundary layer is gradually increased so that it covers the roughness elements so their effect will be negligible.

According to the values of Table 7, total loss of efficiency due to the roughness of stator and rotor is approximately equal to the loss of efficiency due to the roughness of whole stage. This represents a direct dependency of efficiency to increase profile loss due to roughness. Also the effect of increasing stator blade roughness on efficiency is slightly more than the rotor due to its location at the turbine inlet.

In Fig. 16 and 17, loss coefficients of the first and second stators in terms of different pressure ratios are given respectively. It is clear that by increasing height of roughness elements, loss coefficients that are results of flow losses, are increased.

Table 5. Inlet flow rates to the turbine and cooling holes in the roughness of 500 microns (kg/s)

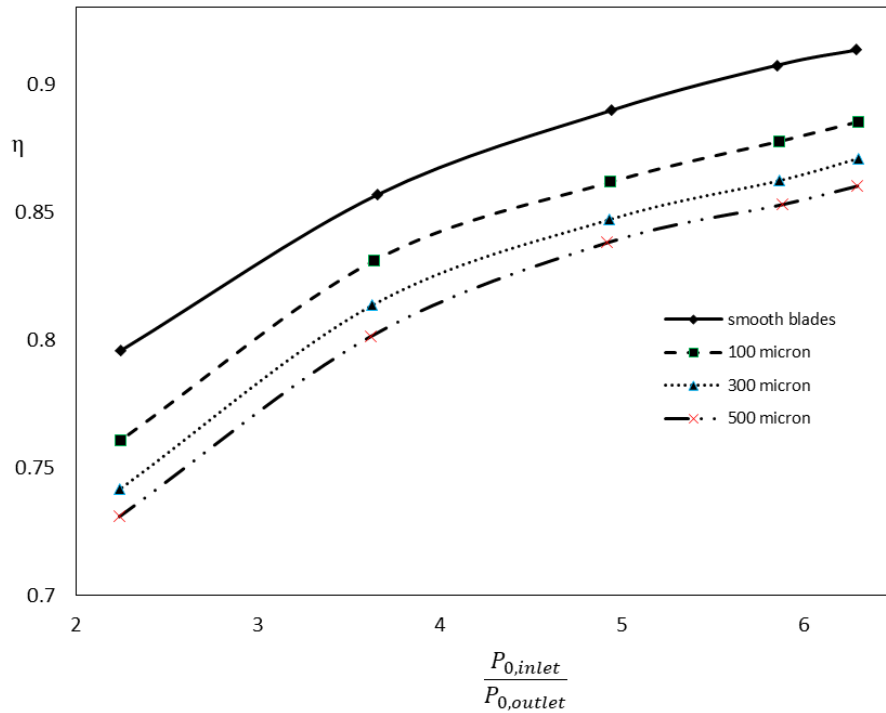| Holes of rotors	Holes of the second stator	Holes of the first stator	Turbine inlet	Pressure ratio
0.2800	0.5859	1.2735	9.9864	5.55

Fig. 15. Turbine efficiency versus total to total pressure ratio for different roughness values

Table 6. Turbine efficiency in case of smooth and different roughness

Turbines with 500 micron roughness	Turbines with 300 micron roughness	Turbines with 100 micron roughness	Normal turbine	$\dfrac{P_{t,i}}{P_{t,o}}$
0.8601	0.8710	0.8853	0.9134	8
0.8529	0.8623	0.8776	0.9074	7
0.8380	0.8470	0.8617	0.8898	5.55
0.8012	0.8135	0.8309	0.8567	4
0.7307	0.7414	0.7605	0.7957	2.5

Table 7. Turbine efficiency in smooth mode, rough stator and rough rotor

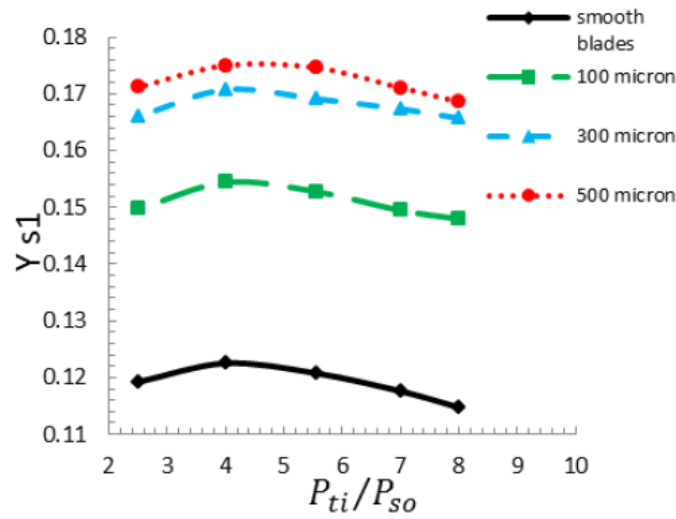| Stator and rotor with 300 micron roughness	Rotor with 300 micron roughness	Stator with 300 micron roughness	Turbine with smooth blades	$\dfrac{P_{t,i}}{P_{t,o}}$
0.8710	0.8979	0.8802	0.9134	8
0.8623	0.8919	0.8766	0.9074	7
0.8470	0.8742	0.8613	0.8898	5.55
0.8135	0.8411	0.8285	0.8567	4
0.7413	0.7802	0.7566	0.7958	2.5

Fig. 16. Loss coefficients of the first stator for smooth and rough modes.
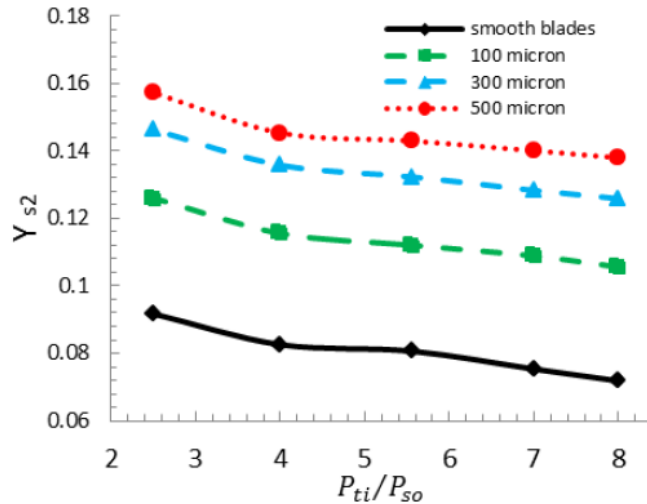

Fig. 17. Loss coefficients of the second stator for smooth and rough modes.

Loss coefficient represents the energy which is lost due to friction and its effect is shown by pressure drop and temperature drop. It is obvious that in stator, loss coefficient changes with a small rate that according to Equations 6 and 7 indicates a slight impact of total pressure ratio of turbine on first stage and first rotor.

In Fig. 18 and 19, loss coefficients are presented in smooth and rough rotors. According to Fig. 18 and 19, the loss coefficients of the first rotor are the maximum and in second rotor, the rate of increase in loss coefficient is very high. This is because of the

losses caused by the rotor blades tip clearance and secondary flows in the rotor.

In low pressure ratios, because of the low mass flow rate and depreciation of flow in the turbine outlet there is a severe shortage of flow energy. This trend by increasing pressure ratio after the design point is reduced, after the design point energy of flow reaches a value that effects of the losses are reduced. Intense increase in loss coefficient in pressure ratios before the design point and then reduction in rate of increase after the design point in the second rotor can be one of the factors that affect the trend of efficiency variations.
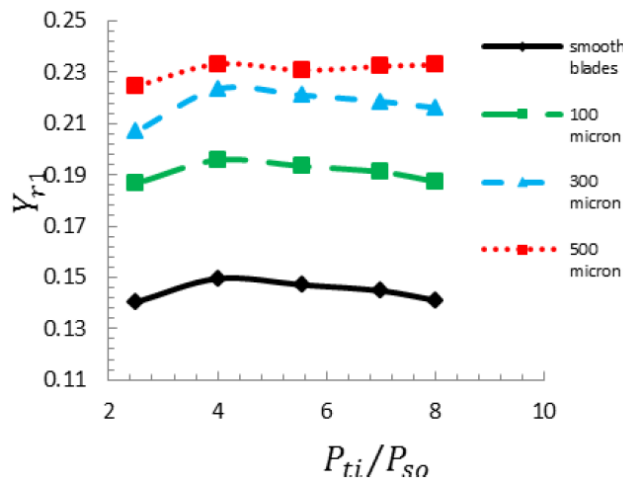
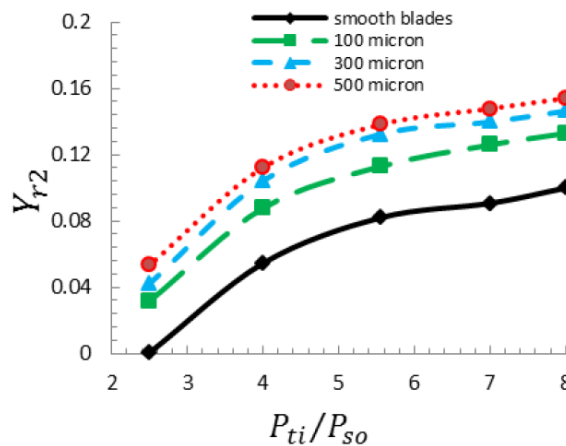**Fig. 18.** Loss coefficients of the first rotor for smooth and rough modes.

Fig. 19. Loss coefficients of the second rotor for smooth and rough modes.

8. Conclusions

In this study, the E^3 turbine is simulated three-dimensionally and the numerical results are validated with the experimental results. Then the effects of blade roughness on the flow field and turbine performance at five different pressure ratios are investigated. The results of this research can be mentioned as the following.

Although by increasing the roughness, the turbine efficiency is reduced but this obvious result is not considered in this study and detection of fluid flow through the turbine to create this reduction, is performed.

In the rough mode, the roughness elements are outside from the viscous sublayer and drag force that is created by these elements caused the extreme increase of friction. By increasing the height of roughness elements, the thickness of the boundary layer also increased especially at suction side and caused greater loss of the profile. By increasing the thickness of the boundary layer, rotation of velocity vectors of the rotor are reduced. It means that the rotor critical angle will be different with the design value.

Total loss of efficiency due to the roughness of stator and the rotor is approximately equal to the loss of efficiency due to the roughness of the stage that this indicates a direct dependence of efficiency to increase profile loss due to the roughness. Also the impact of increasing roughness of the stator blades on efficiency, because of its place at turbine inlet is slightly more than the rotor.

Considering the existence of two stages of the turbine and obtained results, there are major differences between the results of loss coefficients of the first and second stages. This

difference is due to influence of the first stage on the second stage. At inlet of turbine where the boundary layer thickness is not able to cover roughness elements, flow has been extremely affected and desired arrangement of stream lines is disturbed. Also the flow through the turbine especially in the boundary layer is affected by the tip clearance of the rotor blades and the rotor rotational motion. In addition, the stream that has passed the first stage and transferred the amount of energy to the first rotor blades and its temperature decreased, has not desirable arrangement on the second stage and is not able to overcome destructive factors such as roughness, thus, part of the initial energy of the fluid will not be transferred to the rotor blades and turbine efficiency will be reduced.

The role of cooling flow of blades to prevent the effects of high temperatures on components of turbine and also improve the turbine efficiency is undeniable but incoming cooling air into the boundary layer is one of the factors that increasing the thickness of the boundary layer and will lead to increase the profile loss. Optimal adjustment of the number, location, temperature and inlet cooling rate of the holes, has highlighted the effective role of these holes in comparison with the negative role of them. In addition, with the creation of defects and especially roughness, fluid temperature will be restored under the influence of friction and following heat transfer, the overall temperature of the turbine during operation, will be significantly increased that the need for cooling will be inevitable.

According to the results can be achieved the considered roughness. According to location, communication and economic conditions that are obtained in this study between different roughness, efficiency and pressure ratio, by achieving considered performance of turbine, attempting to do repair or replacement of components, will be necessary.

In comparison the results of normal and defective turbines, decreasing trend of difference between normal and defective turbine curves have been impressive as in all of them with slight roughness till transition region, variations are drastic and then gradually by increasing roughness, are reduced. As a result, in order to save costs, the

smallest defects in the industry should be taken seriously.

References

[1] Thakker A., Frawley P., Khaleeq H.B., Abugihalia Y., Setoguchi T., "Experimental and CFD Analysis of 0.6m Impulse Turbine with Fixed Guide Vanes", Proceedings of the 11th international offshore and polar engineering conference, Stavanger, Norway,2001.
doi: ISOPE-I-01-094

[2] Hudson S.T., Zoladz T.F., Dorney D.J., "Rocket Engine Turbine Blade Surface Pressure Distributions: Experiment and Computations", Journal of Propulsion and Power, Vol. 19, No. 3, 2003, pp. 364-373.
doi: 10.2514/2.6140

[3] Aghaei tog R., Tousi A.M. , "Design of Turbine Test Rig for Satellite Launch Vehicle Engines by Using Gas Dynamic Modeling Method", IAS2009-PR-235, February , 2009.

[4] Aghaei tog R., Tousi A.M., Tourani A., "Comparison of Turbulence Methods in CFD Analysis of Compressible Flows in Radial Turbomachines", Journal of Aircraft Engineering and Aerospace Technology, Emerald, London,Vo.l80, Issue 6, 2008, pp.657 - 665.
doi: 10.1108

[5] Fiala. A., Kugeler, "Roughness Modeling for Turbomachinery", Proceedings of ASME Turbo Expo, Vancouver, British Columbia, Canada, June 2011.
doi:10.1115/GT2011-45424

[6] Stripf M., Schultz A., Bauer H.J., "Roughness and Secondary Flow on Turbine Vane External Heat Transfer", Journal of Propulsion and Power, Vol.23, No.2, 2007, pp 283-291.
doi: 10.2514/1.23062

[7] Young –Seok Kang, Jae-Chun Yoo,Shin-Hyoung Kang,2004, "Numerical Study of Roughness Effects on a Turbine Stage Performance", Proceedings of ASME Turbo Expo, Power for Land, Sea, and Air, June 14-17, Vienna, Austria,2004.
doi:10.1115/GT2004-53750

[8] Hummel F., Lötzerich M., Cardamone P., Fottner L., "Surface Roughness Effects on

Turbine Blade Aerodynamics", Proceedings of ASME Turbo Expo, Power for Land, Sea, and Air, Vienna, Austria, June 14-17, 2004.
doi:10.1115/1.1860377

[9] Aligoodarz M. R., Karrabi H., Soleimani Tehrani M. R., "Study and Analysis of Blade Twist, Lean and Bow Effects on the Axial Turbine Performance", Modares Mechanical Engineering Journal, Vol. 12, Issue 4, 2012, pp.9 - 20.

[10] Menter, F. R., "Two-Equation Turbulence-Viscosity Turbulence Models for Engineering Applications" AIAA Journal. Vol. 32, No. 8, 1994, PP 1598-1605.
doi: 10.2514/3.12149

[11] Montis, M., Niehuis, R., Fiala, A., 2010, "Effect of Surface Roughness on Loss Behavior, Aerodynamic Loading and Boundary Layer Development of a Low-Pressure Gas Turbine Airfoil", Proceedings of ASME Turbo Expo, Glasgow, UK, June 14-18 2010.
doi:10.1115/GT2010-23317

[12] Halila EE. Lenahan D.T., Thomas T.T, "Energy Efficient Engine high pressure turbine test hardware detailed design report", NASA CR-167955, 1987.

[13] Yun, Y., Park, Y., Song, S., , "Performance Degradation Due to Blade Surface Roughness in a Single-Stage Axial Turbine", Proceedings of ASME Turbo Expo, Power for Land, Sea, and Air, Vienna, Austria, June 14-17, 2004.
doi:10.1115/1.1811097

[14] ANSYS Help Document, ANSYS CFX-Pre User's Guide, Release 14.5.

[15] Heidari Nejad GH., "Advanced Fluid Mechanics",Tehran, SID Publications ,2005.